Ann. Rev. Pharmacol. Toxicol. 1981. 21:549–73

STEREOLOGY: APPLICATIONS TO PHARMACOLOGY

◆6806

Robert P. Bolender

Department of Biological Structure, University of Washington, School of Medicine, Seattle, Washington 98195

INTRODUCTION

The trend in pharmacological problem solving is clearly moving in the direction of collecting more and more detailed information, which in turn is being called upon to evaluate the effectiveness and safety of drugs. Any information explosion, similar to the one now occurring, is expected to generate a healthy debate regarding the collection and use of such information, and the purpose of this review is to look at some of the problems—related to interpreting information—that we may be facing in the future. The scope of the discussion has been simplified somewhat by restricting it to a consideration of several possible "answers" to a single question, namely: What are we measuring when we measure a change?

Pharmacologically induced changes in cells represent very complex events. When setting out to study such changes, we are confronted not only by the task of choosing "good" questions, but also by the far more challenging one of finding correspondingly "good" answers. If "good" is defined as something having "accuracy," where accuracy is defined by limits imposed on variables, then complex questions and answers can be reduced to several variables contained within the same equations. Complex information—in this form—can be accommodated in a variety of ways, but one that has gained increasing attention in recent years has been that of systems analysis (1, 2). The basic idea of this approach is that a mathematical model for a system is constructed, then an analysis of the model is performed, and, finally, the results are applied to the original system. Ideally, there should be extensive interactions between the construction, the analysis, and the interpretation of the model.

0362-1642/81/0415-0549$01.00

Stereology is of interest to a systems analysis approach because it can be used to attach quantitative values to complex biological structures identified in light and electron micrographs. Cells and their organelles can be characterized in terms of volumes, surface areas, lengths, frequencies, shapes, etc [for overviews of the method see references (3–8)]. Such structures are of interest to us here because they represent highly ordered arrays of molecules, which can also be assayed biochemically. When combined, the structural and functional data can be used to assemble relatively simple, yet surprisingly powerful, information networks. In effect, networks may be thought of as a means for establishing an experimental position from which one can compose questions with an improved confidence. For example, integrated structure-function networks are expected to satisfy the dimensional requirements needed to map the molecular topographies of organelles, to pinpoint the specific cellular responses to one or several xenobiotics, and even to predict genetic events from cytoplasmic changes.

CHANGES IN CELLULAR ORGANELLES

In its simplest form a change can be described by a mathematical relationship in which the values of a dependent variable $f(x_1, x_2)$ are determined by two independent variables x_1, x_2. When interpreting data, it is generally assumed that one of the two independent variables, namely x_2, remains constant and can serve as a reference:

$$f(x_1, x_2) = x_1/x_2. \qquad 1.$$

If we substitute, for example, the volume of an organelle compartment V_i (i = the general case for morphological components) for x_1 and a cm^3 of reference volume V_{ref} for x_2, the familiar volume density equation of stereology results where

$$f(V_i, V_{ref}) = V_i/V_{ref} = V_{V_i} \qquad 2.$$

and

$$\sum_{j=1}^{n} (V_i/V_{ref})_j = 1.0. \qquad 3.$$

Several recent studies (9–12), however, have shown that the V_{ref} is somewhat more complicated than expected in that it consists of at least two variables:

$$f(\overline{V}_c, N_c) = \overline{V}_c \cdot N_c = V_{ref}, \qquad 4.$$

where the average cell volume $\bar{V}_c$ is related to the aggregate volume of the cells V_c and their frequency N_c as shown by the equations:

$$\bar{V}_c = V_c/N_c \quad 5.$$

and

$$N_c = V_c/\bar{V}_c. \quad 6.$$

Substituting Equation 4 into 2 we obtain the more accurate expression:

$$f(V_i, \bar{V}_c, N_c) = V_i/\bar{V}_c \cdot N_c = V_{V_i}. \quad 7.$$

For our purposes here, this equation is particularly useful because it defines a change as a function of three independent variables instead of one variable and one constant (Equation 2). When, for example, one wishes to describe cellular responses to drugs—as opposed to changes in a cubic centimeter of cells—the volume of an average cell is the preferred reference variable. Rearranging equation 7:

$$V_i/N_c = V_{V_i} \cdot \bar{V}_c \quad 8.$$

and substituting Equation 5 [$\bar{V}_{i,c} = V_i/N_c$] we obtain:

$$\bar{V}_{i,c} = V_{V_i} \cdot \bar{V}_c. \quad 9.$$

Note that the reference space index (in this case *c* for cell) has been added to the right of subscript *i*. Returning to the more general form of the equation, we can now define a change in the volume of an organelle compartment *i*—in an average cell—as

$$f(\bar{V}_{i,c}) = V_{V_{i,c}} \cdot \bar{V}_c. \quad 10.$$

A similar relationship exists for surface densities

$$f(\bar{S}_{i,c}) = S_{V_{i,c}} \cdot \bar{V}_c \quad 11.$$

and length densities:

$$f(\bar{L}_{i,c}) = L_{V_{i,c}} \cdot \bar{V}_c. \quad 12.$$

At this point, we are faced with a practical problem. Although the estimate for the volume density of Equation 10 is straightforward, an estimate for

the average cell volume more often than not is subject to several experimental errors and restrictions (7, 8, 12). One way around this problem has been to use as a reference the surface area of an organelle compartment—in an average cell—that does not change (9–14). In effect, such a solution allows us to use Equation 10 to estimate *relative* changes in average cells:

$$\bar{V}_{i,c}[E]/\bar{V}_{i,c}[C] = V_{V_{i,c}}[E]/V_{V_{i,c}}[C] \cdot \bar{V}_c[E]/\bar{V}_c[C], \qquad 13.$$

where $[E]$ identifies the experimental values and $[C]$ those of the control. The average cell volume problem can be accommodated by the following relationships, which were developed earlier (10):

$$\bar{V}_c[E]/\bar{V}_c[C] = N_c[C]/N_c[E] = I_{ref}[C]/I_{ref}[E], \qquad 14.$$

where I_{ref} equals the number of intersections between a linear probe in a stereological test system and the underlying profiles of a reference membrane [see, for example, Figure 2 in ref. (9)]. By substitution into Equation 13 one obtains the following relationship:

$$\bar{V}_{i,c}[E]/\bar{V}_{i,c}[C] = V_{V_{i,c}}[E]/V_{V_{i,c}}[C] \cdot N_c[C]/N_c[E]. \qquad 15.$$

Operationally, the frequency ratio ($N_c[C]/N_c[E]$) keeps the number of cells, which are being used to estimate the volume densities, the same for both the control and experimental time points. In this way the unwanted effect of the reference variable N_c as shown in Equation 7 can be neutralized. Equation 15 and its surface and length density counterparts are particularly helpful because they can provide average cell data for cellular populations containing binucleated cells (11) and for cells with pleomorphic nuclei (9).

The development thus far has taken us to where we can now describe what is happening morphologically to an organelle compartment in an average cell. The advantage of the average cell versus either a gram or cubic centimeter of tissue as the reference variable is seen experimentally as a substantial increase in the accuracy of stereological data (12) (Figure 1). Biochemical data, originally referenced to a gram of tissue or a milligram of protein, can be fitted very comfortably into this "average cell framework" and can benefit from a similar increase in accuracy (Figure 1). Notice, however, that the largest gains in experimental accuracy were achieved only after the stereological and biochemical data could be interpreted as a single, interrelated unit of information.

INFORMATION NETWORKS

To this point the definition for changes occurring in the volume of an organelle compartment has been restricted to the behavior of only three

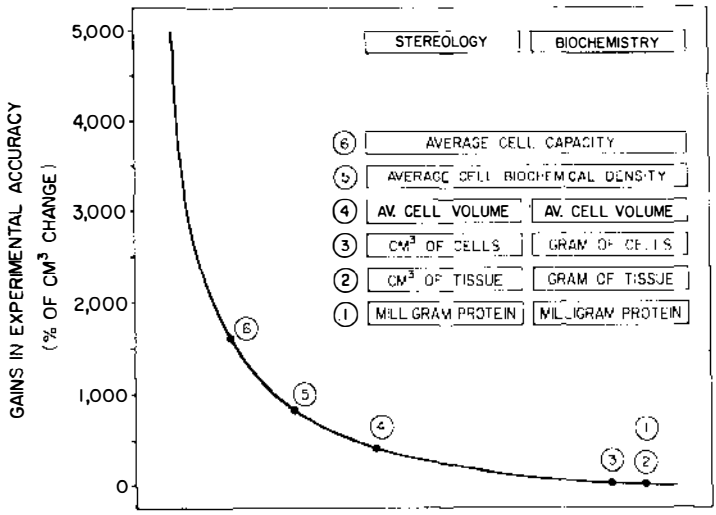

Figure 1 Illustrated are the effects of reference systems and the integration of stereological and biochemical data on experimental accuracy. These results were taken from references (9–12) and Footnotes 1 and 2.

independent variables (Equation 7). In fact, these variables represent merely a small segment of a much larger network of variables. A portion of such a network was constructed to evaluate the effects of phenobarbital on membranes of the endoplasmic reticulum (ER) found within hepatocytes (Figure 2). Here the variables (enclosed by circles) are related to one another by equations (indicated by interconnecting lines). Note that the network has multiple entry and exit points and that biochemical constituents can be related quantitatively to morphological components at several locations. Although several variables were needed, even in such a simple network, most of them serve the primary purpose of transferring information from one part of the network to another. In formulating questions, for example, related to changes in the molecular structure of the membranes, only two variables were required. The first variable defined the amount of a biochemical constituent (BC) contained either within a unit of membrane volume (V_{ref}) or distributed across a unit of surface area (S_{ref}). Such relationships of structure to function are termed biochemical densities (BD) and are described by the following equations:

$$f(BC_i, V_{ref}) = BC_i/V_{ref} = BD_{i,V_{ref}} \qquad 16.$$

and

$$f(BC_i, S_{ref}) = BC_i/S_{ref} = BD_{i,S_{ref}} \qquad 17.$$

Note that ι (iota) is used as the general case for biochemical constituents. The second variable defined the amount of the biochemical constituent contained within an average cell:

$$f(BD_{\iota,V_{ref}}, \overline{V}_{i,c}) = BD_{\iota,V_{ref}} \cdot \overline{V}_{i,c} \quad 18.$$

and

$$f(BD_{\iota,S_{ref}}, \overline{S}_{i,c}) = BD_{\iota,S_{ref}} \cdot \overline{S}_{i,c}. \quad 19.$$

CELLULAR HETEROGENEITIES

The approach just described for studying changes in cells and their organelles may seem overly complicated, but in fact it represents an attempt to match the complexity of the questions being directed at the liver (15). A major pattern in most experimental situations is that cells within the "same population" exhibit remarkable differences in both their structure and function. In the case of hepatocytes, for example, these differences are thought to reflect at least to some extent microenvironmental gradients of nutrients and oxygen (16); hepatocytes at the periphery of the liver lobule receive the blood first, whereas centrolobular hepatocytes receive it last. The literature contains many studies describing zones of hepatocytic differences in both morphology (17–19) and biochemistry (20–24) as well as in the responses of these cells to drugs and toxins (25–31).

But what are the effects of the experimental methods on the detection of these zonal differences? When livers are homogenized in preparation for biochemical assays or when the intact hepatocytes are characterized stereologically, a large proportion of these differences are "lost." The reason for this is that both techniques effectively "homogenize" the information and provide only averaged values. If one considers the inherent differences among hepatocytes as well as the ability of these cells to respond differently to various experimental treatments, it is not surprising that both morphological and biochemical data are often subject to many difficulties of interpretation. A further pattern of complexity is appearing. Fundamental to the interpretation of many enzymatic changes in the liver has been the widespread use of marker enzymes. The assumption, as described by DeDuve (32), has been that the marker enzymes bound to the membranes are uniformly distributed at single morphological (organelle) locations. A substantial literature has now accumulated indicating that marker enzymes can be heterogeneously distributed at single (25, 33–40) and at multiple morphological locations (41–47). While the experimental problems associated with just uncovering the presence of such heterogeneities have been consid-

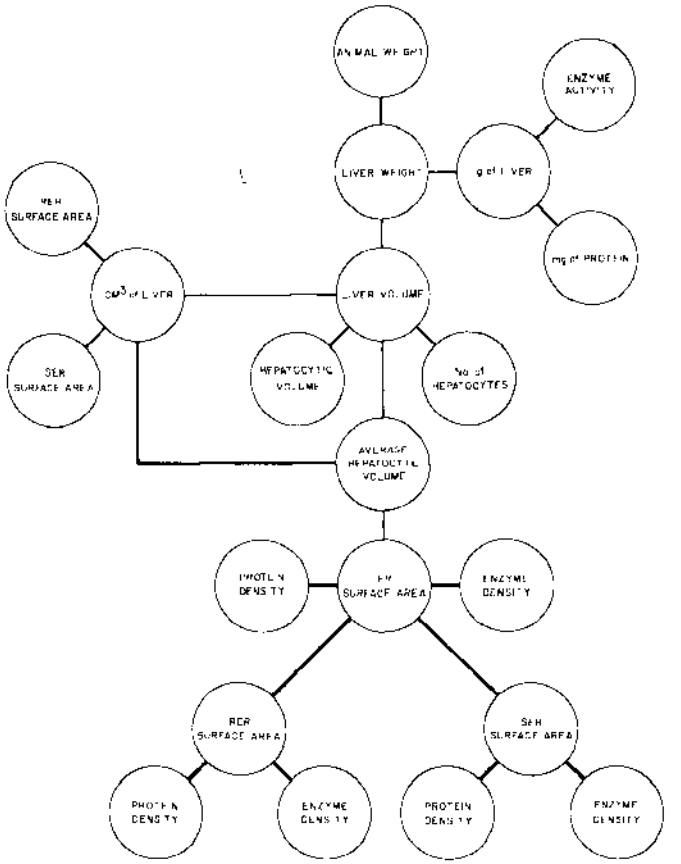

Figure 2 The information network used to study drug induced changes in the membranes of the ER consisted of variables (enclosed by *circles*) connected by equations (shown as *interwening lines*). Note that the volume of an average hepatocyte can be estimated by way of two different pathways. See text for details. From R. P. Bolender et al.[2]

erable, we are now confronted with the more difficult task of finding spatial explanations for them.

A rapidly developing area of research is the study of intracellular distributions of membrane bound marker enzymes. The locations of specific enzymes can be visualized electron microscopically by preparing ferritin labeled antibodies to specific membrane proteins (37, 38, 41, 45, 46). Although the sensitivity of these methods for locating the positions of marker enzymes on membranes is often excellent, this remarkable information has not yet been used to construct areal distribution maps for enzymes in

membranes. Instead of characterizing membrane constituents by estimating particle (i.e. ferritin) densities, nearest neighbor distances, or distribution patterns (48, 49), attention to have been focused on determining whether or not a membrane "appears" to be homogeneous or heterogeneous. Cytochemical approaches provide similar qualitative information, and recent studies have also been quite successful in locating a single marker enzyme at several different morphological locations (42–44, 47, 50). But, once again, the information was not used topographically. Sophisticated methods of centrifugation have also revealed the presence of widespread heterogeneities for membrane bound enzymes (32, 35, 51).

Interhepatocytic heterogeneities are likewise being studied using cell separation systems, and many differences among hepatocytes have been identified (24, 27, 30, 39). Stereologists, however, have approached the problem of interhepatocytic heterogeneities by collecting data directly from the lobular zones: i.e. periportal, midzonal, and centrolobular (17, 19, 31). The major problem here seems to be knowing (*a*) where these zones actually are in the lobule under both control and experimental condition and (*b*) how to weigh the data of each zone in order that they are representative of the entire liver lobule.

Fortunately, sorting differences within and between hepatocytes is a natural extension of the information network (Figure 2), and we now consider the problem of detecting changes in organelle proteins and marker enzyme activities. At the same time, we can "interpret" the same sets of experimental data vis-à-vis different reference variables in order to illustrate how information can be lost or retained. Finally, the efficiency of the integrated approach needs to be demonstrated.

PROTEIN INDUCTION WITH PHENOBARBITAL

Perhaps the most widely known effect of phenobarbital (PB) is the induction of an increased capacity of hepatocytes for metabolizing the drug. The response involves both an increase in the surface area of the ER (11, 52–54) and in the amount of drug metabolizing enzymes (22, 29, 35, 39, 55–60). The protein content of a gram of liver, however, actually decreases slightly during the phenobarbital induction.[1] If we rewrite Equation 7 for protein (Pr) using either a gram as a reference variable (1 cm^3 of liver weighs 1.067 g):

$$f(Pr_{i,g}) = Pr_i/N_c \cdot \bar{V}_c \cdot 1.067\ g(cm^3)^{-1}, \qquad 20.$$

[1]Bolender, R. P. 1981. Systems analysis applied to hepatocytes. II. The effect of phenobarbital on the protein content of organelles and cells. Submitted.

or a volume reference variable:

$$f(Pr_{i,c}) = Pr_i/N_c \cdot \bar{V}_c, \qquad 21.$$

the reason for the decrease can be readily identified. The experimental result is explained by the fact that the cells synthesizing the new membranes simply enlarge, thereby enabling fewer and fewer of them to fit into a gram (or cubic centimeter) of liver (14 and Footnote 2). The decrease in protein is therefore nothing more than an interpretative distortion produced by the N_c reference variable. If, instead, the changes in protein are interpreted with respect to the volume of an average cell, one readily finds the expected increases.

Our purpose at this point is twofold: (*a*) to characterize the protein concentration in the ER membrane in terms of a protein density (PrD) and (*b*) to determine the amount of this protein in an average cell, according to Equations 16 and 18. The usual approach in estimating the protein content of a membrane involves sophisticated purification methods which depend largely on the behavior of membrane vesicles in centrifugal fields [for a discussion see reference (61)]. If, instead, we use the stereological data collected from the intact tissue and the protein assays from the liver homogenates (for both control and phenobarbital treated animals) similar estimates for the protein content of the ER can be obtained. The procedure, described in detail elsewhere[2] consists merely of solving several sets of simultaneous equations. The general equation is given as:

$$f(PrD_a,\ V_a,\ PrD_\beta,\ V_b) = V_{a+b}(PrD_{\alpha+\beta}) = V_a(PrD_\alpha) + V_b(PrD_\beta), \qquad 22.$$

where α indexes one protein density and β the other, which are associated with the corresponding morphological compartments a and b. If we substitute RER for a, SER for b and ER for a + b, the equation can be read as follows: The volume of the ER (e.g. in cubic micrometers) times the protein density of the ER membrane (e.g. milligrams of protein per cubic micrometer) equals the sum of the products of its two subcompartments. In other words, the protein of the ER is equal to the sum of the RER and SER protein. Since the equations involve only two unknowns ($PrD_{\alpha,\beta}$) their solution can be illustrated graphically as the point(s) at which the equations intersect (Figure 3). Note that in this case all six equations share a single solution, which suggests that the original protein content of the RER and SER—in an average hepatocyte—is maintained at a remarkably constant

[2]Bolender, R. P., Barlow, S., White, M. 1981. Systems analysis applied to the liver. I. The effects of phenobarbital on the distributions of ER marker enzymes in hepatocytes. Submitted.

level throughout the PB treatment period. Moreover, these estimates, based on Equation 22, are most encouraging in that they compare favorably to those obtained using the purification approaches.[1] There is a second, and perhaps far more interesting piece of information contained in Figure 3. Given what we have come to accept as inevitable "biological variation," it is most surprising to uncover a biological result so exact. Note that the solution involves data collected from ten animals and that it appears at the end of several thousand calculations. Apart from reporting this result as an indication that the hepatocyte enjoys a remarkable mechanism for controlling the amount of protein in its ER membranes, what can Figure 3 tell us about the mechanism itself?

In 1947, Dantzig (62) introduced the simplex method for linear programming, which made it possible to deal with large numbers of variables simultaneously. In recent years, it has become one of the most frequently and successfully applied mathematical methods in business and industry for allocating resources in a manner such that profits are maximized. The method is of interest to us here because it relies on a calculative scheme similar to the one that we have just used to estimate protein densities for the RER and SER. Consequently, all we need to do at this point is to restate our question as a linear programming problem. We know that an average

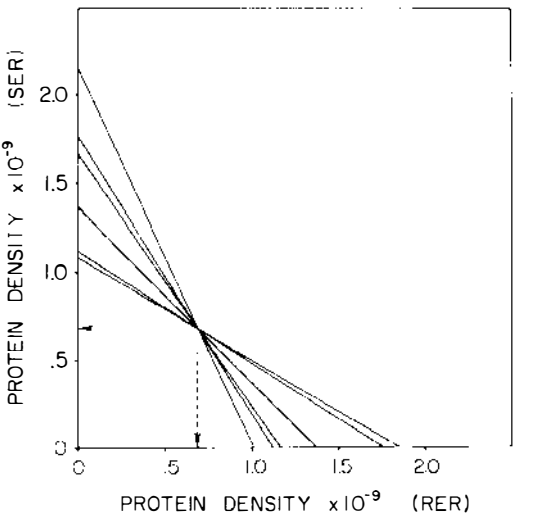

Figure 3 The six linear equations represent data collected from control and PB treated animals; see Equation 22 in text. The simultaneous solution of these equations locates the protein densities for the SER and RER (*arrows*). Details of the experiment are given in Figure 4. From R. P. Bolender.[1]

hepatocyte exposed to PB responds by modifying several of its organelles, which obviously involves shifts in the amount and distribution of its protein resources. More specifically, remodeling of the ER membranes involves increasing the hepatocytic content of drug metabolizing enzymes for which the cell must allocate a certain proportion of its protein synthesizing capacity. We can therefore ask: How much protein is allocated to the RER and SER in order that the average hepatocyte can maximize its response to the PB treatment? The six equations in Figure 3 all have an optimal solution at a single intersection point, which indicates a consistent maximization of the protein allocation. The mechanism for controlling the amount of protein in the RER and SER membranes would therefore seem to be based on a linear programming algorithm. It is, however, very difficult to imagine such a calculation being performed in the absence of a "computer facility," and it may be more than idle speculation to suggest that hepatocytes enjoy extensive information processing capabilities.

Several additional sets of protein and enzymatic data have now been analyzed using linear programming[2] (Bolender, unpublished observations) and patterns of maximization have emerged almost without exception. One practical application of this approach is that it opens the door to an effective management of problems related to cellular heterogeneities.

COHERENCY OF DATA INTERPRETATIONS

This might be a good point in the review to pause for a moment and consider briefly a more general problem related to the interpretation of data. How, for example, can different laboratories do essentially the same experiment and yet arrive at quite different results? The experiment we have been discussing, namely that of phenobarbital induction, has been repeated several times (54, 57, 63), and it might be interesting to look for a partial answer to the question above by considering what it means to use a milligram of microsomal protein as a reference variable for detecting changes in marker enzyme activities. (A microsomal fraction is obtained by differential centrifugation of a liver homogenate, and it contains membrane vesicles derived primarily from the ER.) Figure 4 illustrates the net effects of the reference variable for each of the four studies, and the differences, presumably due to the way in which the microsomes were collected, are very substantial indeed. Comparing relative changes in specific activity (an enzyme activity related to a milligram of protein) given the almost 300% range of the controls therefore seemed less informative than comparing the slopes of the specific activities directly (see, for example, Figure 5). Although all four curves indicate increases in the activity of NADPH cytochrome *c* reductase (one of the enzymes involved in drug metabolism), their

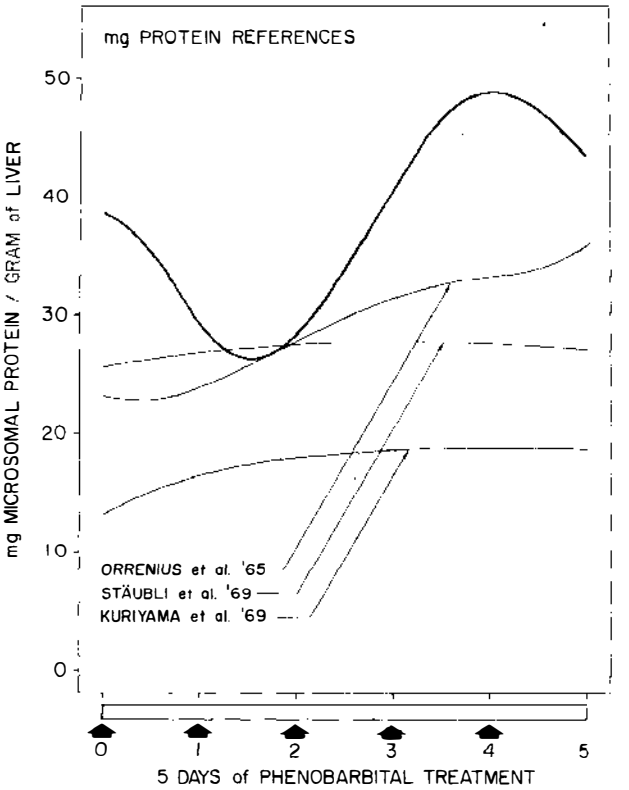

Figure 4 Animals were treated with phenobarbital (PB) for 5 days (100 mg/kg/day; the *arrows* represent the i.p. injection and the *rectangle* the treatment period. The figure illustrates the results of several laboratories, including one from ours (*darker curve*). From R. P. Bolender.[1]

slopes are notably different. A similar pattern is seen for glucose-6-phosphatase (also an ER marker enzyme), except that in this case the slopes are negative (Figure 6). Although the original intent was to run all of the data from Figures 5 and 6 through the equations of the network (Figure 2), in order to demonstrate the effectiveness of an average hepatocyte for producing similar results, the plan could not be implemented because the three earlier studies lacked the key data needed to enter the network.[1] We can, however, still accommodate our original question of data coherency, although provisionally, by asking yet another question: To what extent are microsomal fractions representative of events that are occurring within an average hepatocyte?

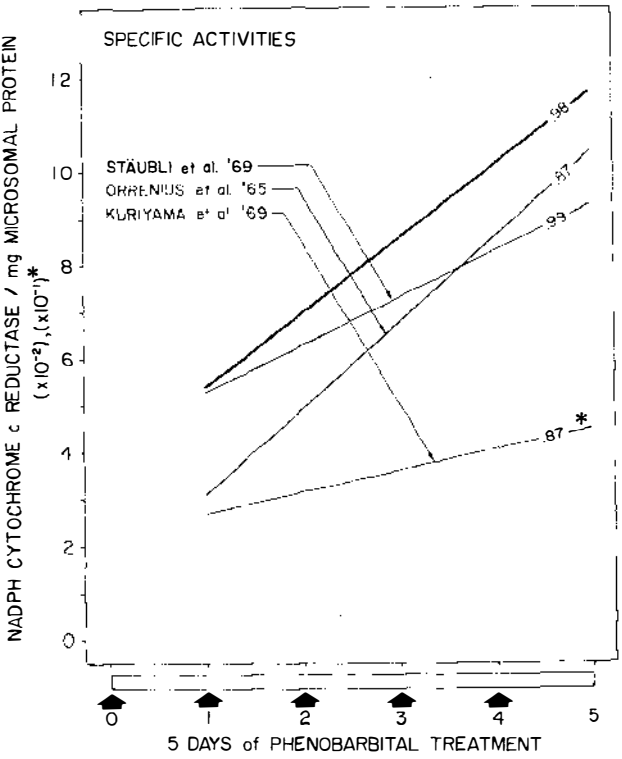

Figure 5 Specific activities for NADPH cytochrome *c* reductase—based on the protein data of Figure 4—were fitted to regression curves; coefficients of determination (r^2) are given. See Figure 4 for details. From R. P. Bolender et al.[2]

Estimates for the relative amounts of RER and SER in a microsomal fraction—or for that matter in any fraction—have been frustrated by the fact that the SER is but one of several "smooth surfaced" membrane compartments, and that a single microsomal vesicle may contain membrane segments from both RER and SER (40). As we shall see in the next section, Equation 26 can be used to estimate the enzyme densities (ED) for both the RER and SER. However, if one already knows these EDs for two different marker enzymes, then the surface areas of the RER (a) and SER (b) in any fraction can be found by simply solving pairs of linear equations simultaneously. A pair of such equations is illustrated below:

$$S_{a+b}(ED_{\alpha+\beta}) = S_a(ED_\alpha) + S_b(ED_\beta) \qquad 23.$$

$$S_{a+b}(ED_{\gamma+\delta}) = S_a(ED_\gamma) + S_b(ED_\delta), \qquad 24.$$

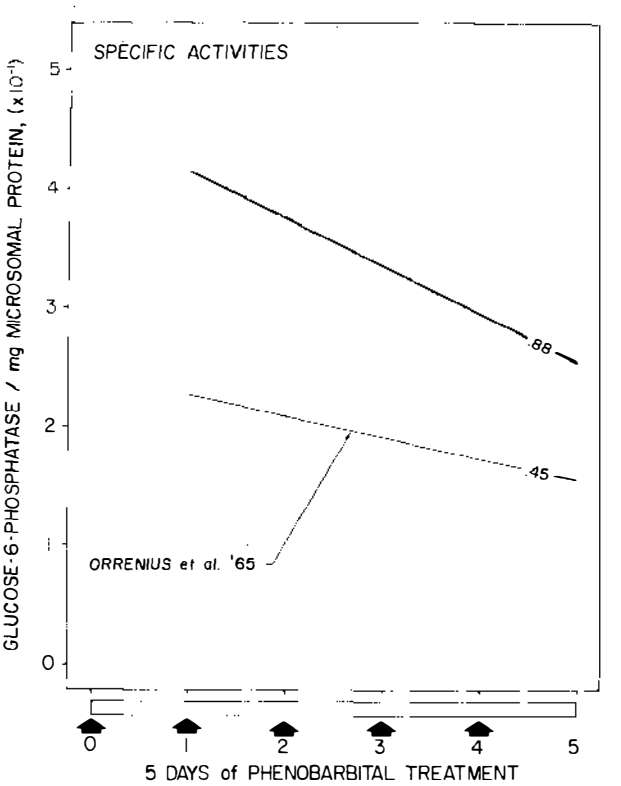

Figure 6 Specific activities for glucose-6-phosphatase are illustrated. See Figures 4 and 5. From R. P. Bolender et al.[2]

where in our case $ED_{\alpha,\beta}$ represents NADPH cytochrome *c* reductase activity/μm^2 and $ED_{\gamma,\delta}$ represents glucose-6-phosphatase activity/ μm^2; S_{a+b} ($ED_{\alpha+\beta}$) and S_{a+b} ($ED_{\gamma+\delta}$) represent the units of enzyme activity found within an average hepatocyte. The solutions to several pairs of these equations (observed values) are given as ratios of surface areas in Figure 7; they are compared to similar ratios predicted by the estimates derived from the intact cells. Note that as the drug induction continued, a progressively larger proportion of the newly synthesized SER membranes were recovered in the microsomal fractions. The conclusion taken from this figure is that the SER/RER membrane ratios of the microsomes, in fact, do not reflect their counterparts in the intact cells. It seems likely, therefore, that the specific activity estimates seen in Figures 5 and 6 are being influenced by (*a*) the protein content of the fraction and (*b*) the way in which the RER and SER membranes have been partitioned. The specific activities of these

microsomal enzymes might be described more accurately by the following equation:

$$f(PrD_i, ED_i, S_i) = \sum_{j=1}^{n} (ED_i \cdot S_i / PrD_i \cdot S_i)_j. \quad 25.$$

ENZYME INDUCTION WITH PHENOBARBITAL

The solution to Equation 25 becomes more complicated when the rough and smooth subcompartments of the ER have different enzyme densities and when these densities are changed in response to the PB treatment. If we eliminate the protein density variable, which is no longer needed, then the enzyme densities for the two subcompartments (a and b) can be estimated by solving simultaneously sets of linear equations:

$$f(S_a, ED_\alpha, S_b, ED_\beta) = S_{a+b}(ED_{\alpha+\beta}) = S_a(ED_\alpha) + S_b(ED_\beta), \quad 26.$$

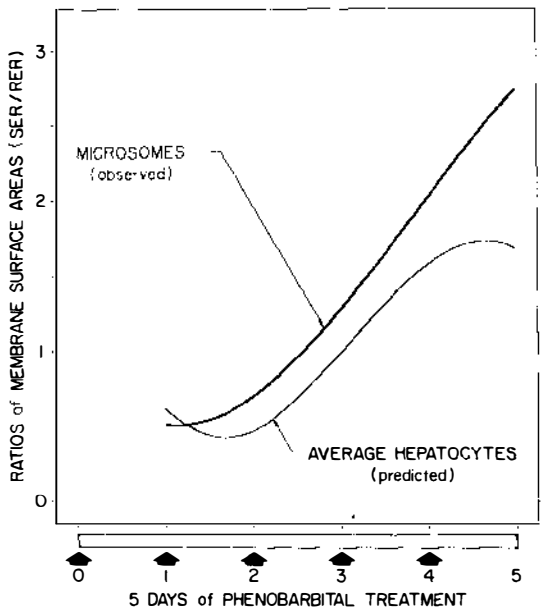

Figure 7 The microsomal ratios (SER/RER), estimated with Equations 23 and 24, indicate that the microsomal fraction becomes less and less representative of the average hepatocyte as the treatment continues. These curves identify a major source of experimental error that can be attributed to the method of differential centrifugation. From R. P. Bolender.[1]

where, in our case, a is the RER, b the ER, and $S_{a+b}(ED_{\alpha+\beta})$ is the activity of an ER marker enzyme measured in the homogenate and related to the volume of an average hepatocyte. In the upper left panel of Figure 8 one can see that the PB treatment caused an initial decrease in the NADPH cytochrome *c* reductase density of the ER, which was followed by a recovery toward the control value. Resolved into the separate effects of the RER and SER subcompartments with Equation 26 (upper right panel) the individual enzyme densities (ED_α and ED_β) displayed pronounced changes during the first day of treatment. The ED of the SER gained 4.8×10^{-13} units of enzyme activity (UEA/μm^2) and the RER lost 6.6×10^{-13} UEA/μm^2. When the EDs are multiplied by the surface areas of their respective membranes, in an average hepatocyte, the enzyme capacity for an average cell ($\overline{EC}_{i,c}$) is obtained:

$$\overline{EC}_{i,c} = \overline{S}_{i,c} \cdot ED_i. \qquad 27.$$

As shown in the lower right panel of the figure, the enzyme capacity of the average hepatocyte, associated with the SER membranes, increased 900% by the end of the treatment period; the RER associated activity decreased to about 50% of its control value. When the SER and RER capacities are added together, one obtains the ER (observed) curve; several solutions of Equation 27, where i = ER, provided the predicted curve. A comparison between the observed and predicted curves served as an independent check for the solutions to the simultaneous equations.

In effect, the enzyme densities of Figure 8 have been used to define quantitatively both biochemical "homogeneities" and heterogeneities. Given the framework of an average cell, both the RER and SER are "homogeneous" at each time point, but they are heterogeneous in the sense that their EDs change. The ER, however, can be considered heterogeneous throughout because it is a composite of variable proportions of RER and SER, both of which display different EDs. Since Figure 8 indicates that the ED of the SER can be as much as 14 times greater than that of the RER, the importance of the SER/RER ratios in the microsomal fraction (Figure 7) with respect to interpreting enzymatic data becomes evident.

The major effect of PB on hepatocytes is generally thought to be related to changes in the electron transport enzymes of the ER. It therefore came as a surprise to discover that glucose-6-phosphatase, an enzyme presumed to be noninducible, displayed changes in activity even greater than those just described for the NADPH cytochrome *c* reductase. The microsomal specific activities (Figure 6) and the ED (upper left, Figure 9) both showed similar downward trends. However, EDs calculated for the RER and SER revealed a marked increase in RER associated activity, whereas the SER

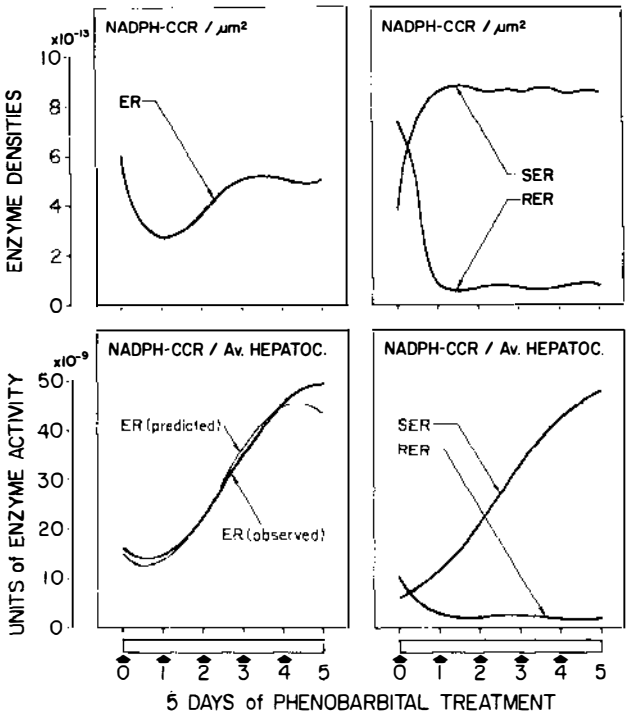

Figure 8 Estimates for the enzyme densities of the RER and SER were based on Equation 26, whereas the enzymatic capacities of an average hepatocyte were estimated with Equation 27. Notice the close agreement between the predicted and observed curves. See text for details. From R. P. Bolender et al.[2]

activity declined. Relative to the volume of an average hepatocyte, the RER associated activity increased by 1600%; this exceeds the NADPH cytochrome *c* reductase SER induction by 400%. Such a result would seem to indicate that PB can also stimulate the synthesis of enzymes involved in carbohydrate metabolism. Indeed, PB seems to have a far more widespread effect on hepatocytes than previously imagined. With the single exception of the surface area of hepatocytic nuclei, everything measured stereologically (ER, mitochondria, Golgi apparatus, peroxisomes, dense bodies) and biochemically (protein, glucose-6-phosphatase, NADPH cytochrome *c* reductase, NADH cytochrome *c* reductase, oxidative demethylase, and P-450)[2] (R. P. Bolender, unpublished observations) were found to be affected by the drug. If, in fact, such an extensive remodeling is a typical cellular response to a xenobiotic substance, then the use of an information network similar to the one described in Figure 2 may offer an attractive means for evaluating the effects of drugs and toxins.

SORTING CELLS MATHEMATICALLY

Thus far, we have focused our attention on events occurring within an average hepatocyte. This "imaginary cell" is the single representative of the more than one billion hepatocytes found within a rat liver. Given the substantial evidence that hepatocytes are heterogeneous with respect to their structure and function, one can begin to appreciate the dimensions and complexity of an experimental design. In practical terms, however, it means that many more variables need to be considered. Equation 7, for example, in a more experimentally rigorous form, would be:

$$f(V_i, V_c) = \sum_{j=1}^{n} (V_i/V_c)_j, \qquad 28.$$

where $j \approx 1 \times 10^9$ hepatocytes. Although such a solution is clearly impractical—it would require collecting measurements from every cell—more ac-

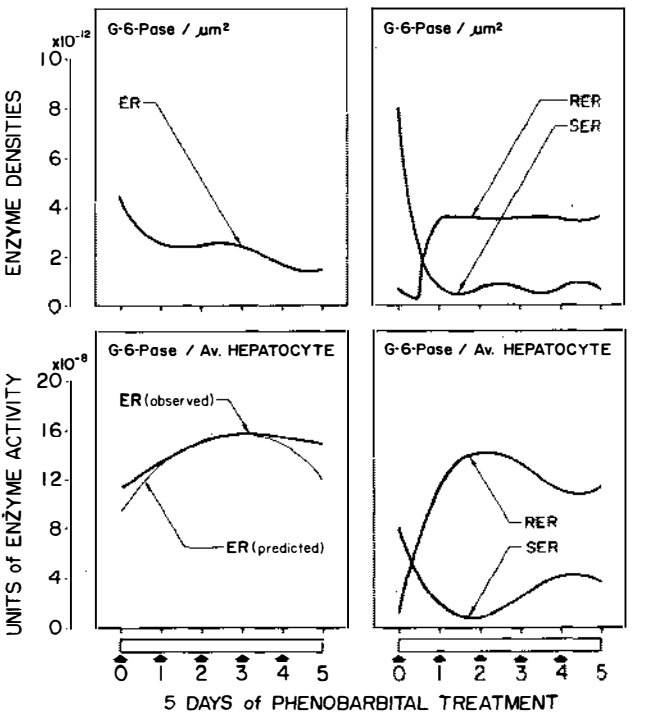

Figure 9 The figure shows changes in glucose-6-phosphatase with respect to the ER membranes and the average hepatocyte. See Figure 8. From R. P. Bolender et al.[2]

ceptable solutions lie somewhere between the limits defined by Equations 7 and 28. The nature of the question being asked determines the value of *j*, and the method for extracting more detailed information from the average hepatocyte, where *j* is equal to 1, once again depends on solving sets of linear equations simultaneously. At this point, however, we find ourselves in a fortunate position because hepatocytes display distinct structural and functional differences. These are exactly the variables needed to sort the hepatocytes into several "homogeneous subpopulations" of average hepatocytes. Accordingly, the *j* of Equation 28 can be reduced to 100, 10, or 1 depending on the experimental goals.

The first step of this sorting procedure is to estimate the number (N) of cells in each subpopulation ($N_1, N_2 \ldots N_n$). The uniqueness of a subpopulation is defined as the ratio of two structural parameters (a/b). The solutions to sets of simultaneous equations provide the frequencies of the subpopulations:

$$f[(a/b)_1, N_1, (a/b)_2, N_2, (a/b)_n, N_n] = (a/b)_1 \cdot N_1 + (a/b)_2 \cdot N_2 + \ldots + (a/b)_n \cdot N_n = \sum_{j=1}^{n} (a/b)_j \cdot N_j, \quad 29.$$

and similarly, the average cell volumes for each subpopulation ($\overline{V}_1, \overline{V}_2, \overline{V}_n$) can be estimated with the following equation:

$$f(N_1, \overline{V}_1, N_2, \overline{V}_2, N_n, \overline{V}_n) = N_1 \cdot \overline{V}_1 + N_2 \cdot \overline{V}_2 + \ldots + N_n \cdot \overline{V}_n = \sum_{j=1}^{n} N_j \cdot V_j. \quad 30.$$

Equations 29 and 30 have already been tested experimentally using suspensions of lymphocytes, an experimental model that permits an independent estimate for the cell frequencies, and the results were most satisfactory (11, 64).

If we now rewrite Equation 7 for surface areas (S_i) using first a unit of volume as a reference variable:

$$f(S_i, \overline{V}_c, N_c) = S_i/\overline{V}_c \cdot N_c = S_{V_c}, \quad 31.$$

and then the average cell volume as the reference variable (see Equations 8–10), we obtain:

$$f(\overline{S}_{i,c}) = S_{V_{i,c}} \cdot \overline{V}_c, \qquad 32.$$

which defines the amount of surface area of a given compartment i in an average cell.

By expanding Equation 31 to include several subpopulations of average hepatocytes and then solving sets of simultaneous equations, one can estimate the total surface areas—S_1, S_2, S_n—in several "homogeneous" subpopulations of cells (recall that the subscript c (cell) was replaced by a numerical index to identify each subpopulation):

$$f(S_1, \overline{V}_1, N_1, S_2, \overline{V}_2, N_2, S_n, \overline{V}_n, N_n) = S_1(\overline{V}_1 \cdot N_1)^{-1} + S_2(\overline{V}_2 \cdot N_2)^{-1} + \ldots + S_n(\overline{V}_n \cdot N_n)^{-1} = \sum_{j=1}^{n} S_j(\overline{V}_j \cdot N_j)^{-1}. \qquad 33.$$

By expanding a condensed version of Equation 26, one can then estimate both structural and functional changes in the cellular subpopulations:

$$f(S_1, BD_1, S_2, BD_2, S_n, BD_n) = S_1 \cdot BD_1 + S_2 \cdot BD_2 + \ldots + S_n \cdot BD_n = \sum_{j=1}^{n} S_j \cdot BD_j. \qquad 34.$$

Equation 34 is a complex expression coming at the end of a long development that began with the two variables (x_1, x_2) of Equation 1. In arriving at this terminus, it appears that a simple relationship has been transformed into a very complex one by adding more and more variables. In fact, however, the development occurred in quite the opposite direction. A simple form of Equation 34 was first found experimentally (see Figures 3, 8, and 9), and only afterward was it used to derive Equation 1. The point to be made here is that "simple" relationships, such as Equation 1, are simple only because all of the information has been condensed into a few variables. Such information is practically useless because all of the interesting details are effectively lost during the process of condensation, i.e. going from Equation 34 to Equation 1.

Under experimental conditions, the Σ portions of Equations 28, 29, 30, 33, and 34 are reduced to a single measurement and the unknown variables

are obtained by solving simultaneous equations. These solutions can be obtained graphically (when only two or three unknowns are present), or they can be calculated directly using the methods of linear algebra or linear programming (65, 66).

CONCLUSION

In the introduction, we began by asking: "What are we measuring when we measure a change?" The question was formulated to focus attention on several problems of interpretation that arise each time we collect information from a biological system. Equations and practical examples were used to illustrate the complexity of a biological change, and an attempt was made to reduce this complexity by characterizing change as a function of several interrelated variables. Essentially, the liver and its multifaceted response to a drug treatment were analyzed using a systems approach, which is known to be an effective means for attacking difficult large-scale problems (1).

The major points of the review can be summarized with Figure 10. Illustrated is an information module consisting of several steps (variables) connected to one another by two conduits (equations), each of which is capable of transferring information within or between levels. It outlines the response of the liver to a drug. The first major point was to demonstrate experimentally that our ability to measure a change is largely related to our position within the module. If we stand on the step marked "liver," then "good" questions can be asked about the liver or its immediate subcompartments, namely, cells and intercellular spaces. But what happens, for example, if we skip the "hepatocytic" step and address a question directly to the organelles? Such an experimental design leads to a substantial drop in accuracy because reaching beyond an adjacent step leads to a forfeiture of the intervening information (this effect is illustrated in Figures 4 and 5; see Footnote 2). By proceeding in a stepwise manner, however, one retains the information needed to direct questions of increasing specificity at each subsequent step. This point was illustrated by the interpretations of the data in Figures 8 and 9, which used the hepatocytic step to identify average hepatocytic sources of biochemical heterogeneities. Likewise, this step proved to be an effective position from which to estimate the protein content of hepatocytic organelles.[2]

Notice that descending and ascending conduits are included in the module. Usually we think of events as occurring in a cause and effect sequence: The drug is recognized by the receptor, information is transferred to the genome, a response is mobilized, and the net effect is drug metabolism. As this response moves downward through the module, it gathers complexity as more and more variables are brought into play. By beginning

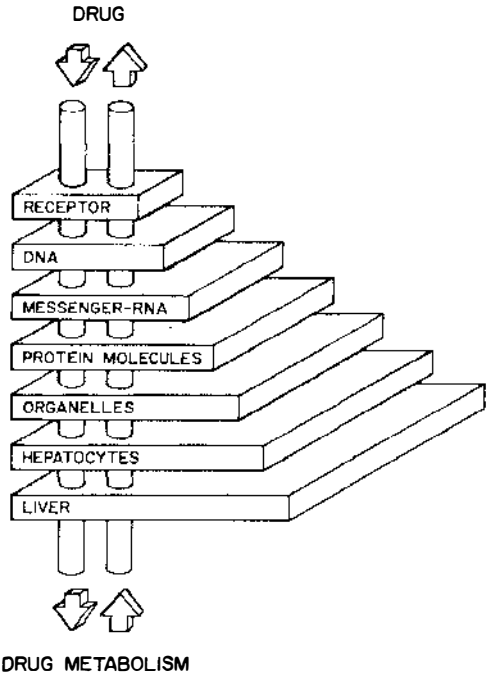

Figure 10 Illustrated is an information module consisting of several steps connected by two conduits. The "liver" is identified as the step containing the greatest amount of information with the "drug receptor" at the other end of the scale. Note that each step contains many substeps, for example, as many as 1×10^9 for the "hepatocytes." Connections between the first three steps have already been found and are defined by the equations given in the text.

the analysis at the most complex end of the module and working upward, however, the sequence is reversed and "effects" can then be used to identify "causes." The advantage of this approach becomes readily apparent when one discovers that taking the next step is much easier than taking the former one. The converse, of course, holds true for the descending conduit.

The second major aim of the review was to consider the problem of lost information. When a liver is homogenized, the ensuing biochemical data are restricted to the first step of the module because most of the organizational information has been lost. Stereological data experience a similar loss when interpreted at this step, but in contrast to chemical data, some of the information can be recovered by moving to a higher step (see for example, Figures 8 and 9). The strategy developed for moving the biochemical data beyond the first step consisted merely of linking them to the morphological data, which already had the required mobility.

Of all the points raised, however, none seems to have the impact generated by Figure 3. Surely, one of the major factors behind a cell's success is its ability to manage very complex information effectively. If we can discover where and how information is processed, then we might be in a better position to understand the mechanisms behind the responses of cells to drugs and toxins. Stereology can contribute to this process of discovery because it has access to an extremely rich network of experimental variables.

ACKNOWLEDGMENT

The preparation of this review and unpublished data was supported by United States Public Health Service Grant GM-22755 from the National Institutes of Health.

Literature Cited

1. Miser, H. J. 1980. Operations research and systems analysis. *Science* 209: 139–46
2. Optner, S. L., ed. 1973. *Systems Analysis.* Baltimore: Penguin
3. DeHoff, R. T., Rhines, F. N. 1968. *Quantitative Microscopy.* New York: McGraw-Hill
4. Elias, H., Pauly, J. E., Burns, E. R. 1978. *Histology and Human Microanatomy.* New York: Wiley
5. Eränkö, O. 1955. *Quantitative Methods in Histology and Microscopic Histochemistry.* Basel: Karger
6. Underwood, E. E. 1970. *Quantitative Stereology.* Reading, Mass: Addison-Wesley
7. Weibel, E. R. 1979. *Stereological Methods,* Vol. I. London: Academic
8. Williams, M. A. 1977. *Quantitative Methods in Biology.* New York: North-Holland
9. Bolender, R. P. 1979. Surface area ratios. I. A stereological method for estimating average cell changes in membrane surface areas. *Anat. Rec.* 194: 511–22
10. Bolender, R. P. 1979. Surface area ratios. II. A stereological method for estimating changes in average cell volume and frequency. *Anat. Rec.* 195: 257–64
11. Bolender, R. P. 1980. Surface area ratios. III. A stereological method for estimating relative changes in average hepatocytes. *Anat. Rec.* 196:323–31
12. Bolender, R. P. 1980. An analysis of stereological reference systems used to interpret drug induced changes in biological membranes. *Mikroskopie.* In press
13. Schaeffer, S. F., Raviola, E. 1978. Membrane recycling in the cone cell endings of turtle retina. *J. Cell Biol.* 79:802–85
14. Schofield, G. C., Ito, S., Bolender, R. P. 1979. Changes in membrane surface areas in mouse parietal cells related to maximal secretion. *J. Anat.* 128:669–92
15. Bolender, R. P. 1979. Morphometric analysis in the assessment of the response of the liver to drugs. *Pharmacol. Rev.* 30:429–43
16. Rappaport, A. M. 1969. Anatomic considerations. In *Diseases of the Liver,* ed. L. Schiff, pp. 1–49. Philadelphia: Lippincott. 3rd ed.
17. Loud, A. V. 1968. A quantitative stereological description of the ultrastructure of normal rat liver parenchymal cells. *J. Cell Biol.* 37:27–46
18. Novikoff, A. B. 1959. Cell heterogeneity within the hepatic lobule of the rat. Staining reactions. *J. Histochem. Cytochem.* 7:240–44
19. Schmucker, D. L., Mooney, J. S., Jones, A. L. 1978. Stereological analysis of hepatic fine structure in the Fischer 344 rat. Influence
animal age. *J. Cell Biol.* 78:319–37
20. Drochmans, P., Wanson, J.-C., Mosselmans, R. 1975. Isolation and subfractionation on Ficoll gradients of adult rat hepatocytes. Size, morphology and biochemical characteristics of cell fractions. *J. Cell Biol.* 66:1–22
21. Katz, N., Teutsch, H. F., Sasse, D., Jungermann, K. 1977. Heterogeneous distribution of glucose-6-phosphatase in

microdissected periportal and perivenous rat liver tissue. *Fed. Eur. Biochem. Soc. Lett.* 76:226–30
22. Koudstaal, J. 1971. *Hydroxyleringen in der rattelever.* PhD thesis. Univ. Groningen, Groningen, Holland
23. Russo, E., Drochmans, P., Penasse, W., Wanson, J.-C. 1975. Heterogeneous distribution of glycogen within the (rat) liver lobule, induced experimentally. *J. Submicrosc. Cytol.* 7:31–45
24. Sasse, D., Katz, N., Jungermann, K. 1975. Functional heterogeneity of rat liver parenchyma and of isolated hepatocytes. *FEBS Lett.* 57:83–88
25. Dallner, G., Ernster, L. 1968. Subfractionation and composition of microsomal membranes: A review. *J. Histochem. Cytochem.* 16:611–32
26. Eriksson, L. C. 1973. Studies on the biogenesis of endoplasmic reticulum and in the liver cell. *Acta Pathol. Microbiol. Scand. Suppl.* 239:1–72
27. Gumucio, J., DeMason, L., Miller, D., Krezoski, S., Keener, M. 1978. Induction of cytochrome P-450 in a selective sub-population of hepatocytes. *Am. J. Physiol.* 234:102–9
28. Lewis, J. A., Tata, J. R. 1973. Heterogeneous distribution of glucose-6-phosphatase in rat liver microsomal fractions as shown by adaptation of a cytochemical technique. *Biochem. J.* 134: 69–78
29. Menard, D., Penasse, W., Drochmans, P., Hugon, J. 1974. Glucose-6-phosphatase heterogeneity within the hepatic lobule of the phenobarbital-treated rat. *Histochemistry* 38:229–39
30. Sweeney, G. D., Jones, K. G., Krestynski, R. 1978. Effects of phenobarbital and 3-methylcholanthrene pretreatment on size, sedimentation velocity and mixed function oxygenase activity of rat hepatocytes. *J. Lab. Clin. Med.* 91:444–54
31. Wiener, J., Loud, A. V., Kimberg, D. V., Spiro, D. 1968. A quantitative description of cortisone-induced alterations in the ultrastructure of rat liver parenchymal cells. *J. Cell Biol.* 37: 47–61
32. DeDuve, C. 1971. Tissue fractionation past and present. *J. Cell Biol.* 50:20D–55D
33. Beaufay, H., Amar-Costesec, A., Thinès-Sempoux, D., Wibo, M., Robbi, M., Berthet, J. 1974. Analytical study of microsomes and isolated subcellular membranes from rat liver. III. Subfractionation of the microsomal fraction by isopycnic and differential centrifugation in density gradients. *J. Cell Biol.* 61: 213–31
34. Bolender, R. P., Paumgartner, D., Muellener, D., Losa, G., Weibel, E. R. 1980. Integrated stereological and biochemical studies on hepatocytic membranes. IV. Heterogeneous distribution of marker enzymes on ER membranes in fractions. *J. Cell Biol.* 85:577–86
35. Dallner, G. 1979. Structural organization of the endoplasmic reticulum. In *The Induction of Drug Metabolism,* ed. R. W. Estabrook, E. Lindenlaub. pp. 133–46. Stuttgart & New York: Schattauer
36. DePierre, J. W., Dallner, G. 1975. Structural aspects of the membrane of the endoplasmic reticulum. *Biochim. Biophys. Acta* 415:411–72
37. Fujii-Kuriyama, Y., Negishi, M., Mikawa, R., Tashiro, Y. 1979. Biosynthesis of cytochrome P-450 on membrane-bound ribosomes and its subsequent incorporation into rough and smooth microsomes in rat hepatocytes. *J. Cell Biol.* 81:510–19
38. Morimoto, T., Matsura, S., Sasaki, S., Tashiro, Y., Omura, T. 1976. Immunochemical and immunoelectron microscope studies on localization of NADPH-cytochrome *c* reductase on rat liver microsomes. *J. Cell Biol.* 68:189–201
39. Sultatos, L. G., Vesell, E. S., Hepner, G. 1979. Heterogeneous response of hepatic mixed function oxidases to chronic phenobarbital administration. *Biochem. Pharmacol.* 28:847–59
40. Wibo, M., Amar-Costesec, A., Berthet, J., Beaufay, H. 1971. Electron microscope examination of subcellular fractions. III. Quantitative analysis of the microsomal fraction isolated from rat liver. *J. Cell Biol.* 51:52–71
41. Borgese, N., Meldolesi, J. 1980. Localization and biosynthesis of NADH-cytochrome b_5 reductase, on integral membrane protein, in rat liver cells. I. Distribution of the enzyme activity in microsomes, mitochondria, and Golgi complex. *J. Cell Biol.* 85:501–15
42. Cheng, H., Farquhar, M. G. 1976. Presence of adenylate cyclase activity in Golgi and other fractions from rat liver. II. Cytochemical localization within Golgi and ER membranes. *J. Cell Biol.* 70:671–84
43. Farquhar, M. G., Bergeron, J. J. M., Palade, G. E. 1974. Cytochemistry of Golgi fractions prepared from rat liver. *J. Cell Biol.* 60:8–25

44. Howell, K. E., Ito, A., Palade, G. E. 1978. Endoplasmic reticulum marker enzymes in Golgi fractions. What does it mean? *J. Cell Biol.* 79:581–89
45. Remacle, J. 1978. Binding of cytochrome b_5 to membranes of isolated subcellular organelles from rat liver. *J. Cell Biol.* 79:291–313
46. Takesue, S., Omura, T. 1970. Immunological similarity between NADH-cytochrome *c* reductase of mitochondrial outer membrane and microsomes. *Biochem. Biophys. Res. Commun.* 40:396–401
47. Widnell, C. C. 1972. Cytochemical localization of 5'-nucleotidase in subcellular fractions isolated from rat liver. I. The origin of 5'-nucleotidase activity in microsomes. *J. Cell Biol.* 52:542–58
48. Pielou, E. C. 1977. *Mathematical Ecology.* New York: Wiley
49. Poole, R. W. 1974. *An Introduction to Quantitative Ecology.* New York: McGraw-Hill
50. Morré, D. J., Ovtracht, L. P. 1977. Dynamics of the Golgi apparatus: Membrane differentiation and membrane flow. *Int. Rev. Cytol. Suppl.* 5:61–188
51. Amar-Costesec, A., Beaufay, H., Wibo, M., Thinès-Sempoux, D., Feytmans, E., Robbi, M., Berthet, J. 1974. Analytical study of microsomes and isolated subcellular membranes from rat liver. II. Preparation and composition of the microsomal fraction. *J. Cell Biol.* 61: 201–12
52. Jones, A. L., Fawcett, D. W. 1965. Hypertrophy of the agranular reticulum in hamster liver induced by phenobarbital (with a review on the functioning of this organelle in liver). *J. Histochem. Cytochem.* 14:215–32
53. Spring-Mills, E., Jones, A. L. 1974. Ultrastructural concepts of drug metabolism. II. The hepatocyte: Phenobarbital and microsomal enzyme induction. *Am. J. Drug Alcohol Abuse* 1:271–98
54. Stäubli, W., Hess, R., Weibel, E. R. 1969. Correlated morphometric and biochemical studies on the liver cell. II. Effects of phenobarbital on rat hepatocytes. *J. Cell Biol.* 42:92–112
55. Brodie, B. B., Gillette, J. R., LaDu, B. N. 1958. Enzymatic metabolism of drugs and other foreign compounds. *Ann. Rev. Biochem.* 27:427–54
56. Conney, A. H. 1967. Pharmacological implications of microsomal enzyme induction. *Pharmacol. Rev.* 19:317–66
57. Kuriyama, Y., Omura, T., Siekevitz, P., Palade, G. E. 1969. Effects of phenobarbital on the synthesis and degradation of the protein components of rat liver microsomal membranes. *J. Biol. Chem.* 244:2017–26
58. Orrenius, S., Das, M., Gnosspelius, Y. 1969. Overall biochemical effects of drug induction on liver microsomes. In *Microsomes and Drug Oxidations,* ed. J. R. Gillette, A. H. Conney, G. J. Cosmides, R. W. Estabrook, J. R. Fouts, G. J. Mannering, pp. 251–70. New York: Academic
59. Orrenius, S., Ericsson, J. I. E. 1966. Enzyme-membrane relationship in phenobarbital induction of synthesis of drug-metabolizing enzyme system and proliferation of endoplasmic membranes. *J. Cell Biol.* 28:181–98
60. Remmer, H., Merker, H. J. 1963. Drug-induced changes in the liver endoplasmic reticulum. Association with drug-metabolizing enzymes. *Science* 142: 1657–58
61. Dallner, G. 1974. Isolation of rough and smooth microsomes—general. In *Methods in Enzymology,* ed. S. Fleisher, L. Packer, 31:191–201. New York: Academic
62. Dantzig, G. B. 1963. *Linear Programming and Extension.* Princeton, NJ: Princeton Univ. Press
63. Orrenius, S., Ericsson, J. I. E., Ernster, L. 1965. Phenobarbital-induced synthesis of the microsomal drug-metabolizing enzyme system and its relationship to the proliferation of endoplasmic membranes. A morphological and biochemical study. *J. Cell Biol.* 25:627–39
64. Bassingthwaighte, E. A., Bolender, R. P. 1978. A morphometric method for obtaining average cell data from cell suspensions. *Anat. Rec.* 190:333
65. Murty, K. G. 1976. *Linear and Combinatorial Programming.* New York: Wiley
66. Weber, J. E. 1976. *Mathematical Analysis: Business and Economic Applications.* New York: Harper & Row